

A Novel Compact Microstrip Balun Bandpass Filter Design Using Interdigital Capacitor Loaded Open Loop Resonators

Ali K. Gorur*

Abstract—A novel microstrip balun bandpass filter (BPF) is designed by using open loop resonators having interdigital capacitors. The interdigital capacitors are employed to control the center frequency easily. Opposite phase difference between the balanced outputs can be provided according to the suitable coupling topologies based on parallel and anti-parallel coupled lines. By this way, minimized magnitude imbalances between the balanced ports can also be obtained. In order to obtain two poles inside the passband, two identical resonators are coupled to each other. The designed balun BPF was fabricated and measured to validate the proposed methodology. Phase and magnitude imbalances inside the passband were measured within $180 \pm 5^\circ$ and 0.5 dB, respectively. The simulated and measured results are in good agreement.

1. INTRODUCTION

Balun bandpass filters (BPFs) have an important place in RF front end modules since they can serve as both of balun and BPF. While a balun converts an unbalanced signal to a balanced signal, a BPF can allow signal transmission at desired frequencies. In a balun BPF, it is desired to obtain a phase difference of 180° between the balanced output ports as well as same magnitudes. Additionally, microstrip structures play an important role in balun BPF designs due to their low loss, low cost, compact size and easy fabrication properties.

In the literature, there are several microstrip balun BPFs designed in various approaches. Dual-mode ring resonators and cross-slotted patch resonator are used to design balun BPFs in [1–3]. In these studies, transmission zeros can be obtained at imaginary and real frequencies depending on the degenerate mode excitations of a dual-mode resonator [4]. Thus, 180° phase difference with almost equal magnitudes can be observed at balanced ports. Standing wave pattern based open-circuited transmission lines are used to design a balun BPF with high performances in [5]. Additionally, capacitively loaded coupled resonators and open loop ring resonators are different approaches to design microstrip balun BPFs [6, 7]. Meanwhile, low temperature co-fired ceramic (LTCC) balun BPF designed in [8] has a multilayer structure constructed by half-wavelength and quarter-wavelength resonators. Substrate integrated waveguides and multi-coupled transmission lines are other methods in balun BPF designs [9, 10].

In this study, a novel microstrip balun BPF is proposed by using open loop ring resonators having interdigital capacitors located at the open ends of the resonators. The proposed topology provides a practical center frequency control mechanism without changing the total circuit size. Center frequency of the passband can be easily controlled by means of the interdigital capacitors. Changes in phase and magnitude imbalances are negligible during the controlling process. Interdigital capacitors are also employed to satisfy compactness in circuit size. In the designed circuit, there are three ports including one unbalanced input and two reciprocally located balanced outputs. Balanced outputs are coupled

Received 9 January 2018, Accepted 16 April 2018, Scheduled 27 May 2018

* Corresponding author: Ali Kursad Gorur (kgorur@nevsehir.edu.tr).

The author is with the Department of Electrical and Electronics Engineering, Nevsehir Haci Bektas Veli University, Nevsehir 50300, Turkey.

to resonators so as to obtain opposite phases and they have almost equal magnitudes. The designed balun BPF has also been fabricated and measured. Measured results are in a good agreement with the simulated ones. Phase and magnitude imbalances inside the passband were measured within $180 \pm 5^\circ$ and 0.5 dB, respectively.

2. DESIGN METHODOLOGY

2.1. Resonator Analysis

The proposed interdigital capacitor loaded open loop resonator is illustrated in Fig. 1(a). As shown in this figure, in order to analyze the proposed resonator, it is coupled to input and output ports by lumped capacitors. It is known that even and odd mode equivalent half circuit models can be obtained by locating magnetic and electric walls to the symmetry axis of the resonator, respectively [11]. The even and odd mode equivalent half circuits are also depicted in Figs. 1(b) and 1(c), respectively. Here, θ and Z_0 represent electrical length and characteristic impedance of the related transmission lines, respectively. Also, C_g and C_{int} describe coupling and interdigital capacitors, respectively. Capacitance of an interdigital capacitor can be calculated according to the formula given in [11]. From Fig. 1(b), even mode input impedance may be expressed as,

$$Z_e = \frac{1}{j\omega C_g} + \frac{-jZ_{01}Z_{02}}{Z_{02} \tan(\theta_1) + Z_{01} \tan(\theta_2)} \quad (1)$$

where subscripts 1 and 2 represent the upper and bottom parts in Fig. 1(b). Odd mode input impedance can also be derived according to Fig. 1(c) as,

$$Z_o = \frac{1}{j\omega C_g} + Z_r \quad (2a)$$

$$Z_r = \frac{-jZ_{01}Z_{02}(1 - \omega C_{int}Z_{01} \tan(\theta_1))}{Z_{01} \cot(\theta_2)(\omega C_{int}Z_{01} \tan(\theta_1) - 1) + Z_{02}(\omega C_{int}Z_{01} + \tan(\theta_1))} \quad (2b)$$

It is clear that the interdigital capacitors are only effective on the odd mode resonance frequency. Hence, center frequency adjustment mechanism can be achieved through the odd mode of the resonator. As well known, even and odd mode resonance conditions can be obtained by equating Z_e and Z_o to zero [11].

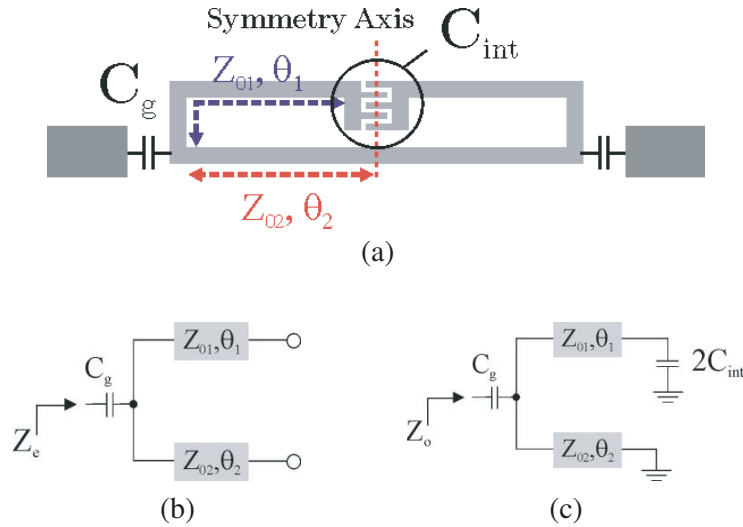


Figure 1. (a) Proposed interdigital capacitor loaded open loop resonator, (b) even mode equivalent circuit model, (c) odd mode equivalent circuit model.

2.2. Balun BPF

The proposed microstrip balun BPF is shown in Fig. 2(a). As can be seen from the figure, interdigital capacitor loaded open loop resonators are coupled to input and output ports by means of open ended feedlines. It should also be noted that there are two interdigital capacitor loaded open loop resonators with identical electrical lengths in order to obtain two poles inside the passband. Since they are coupled to each other capacitively, coupling scheme of the proposed balun BPF can be constructed as indicated in Fig. 2(b). As can be seen from this figure, unbalanced input port is coupled to the first resonators, and these resonators are also coupled to balanced output ports. As in [7], locations of the balanced output ports are decided so as to obtain a phase difference of 180°. Maximum magnetic coupling can be observed in the middle of the bottom sides of the resonators, whereas electric coupling can be observed at the interdigital capacitors. This situation can also be seen from the current and charge distributions of the designed topology as depicted in Figs. 3(a) and 3(b), respectively. Another significant advantage

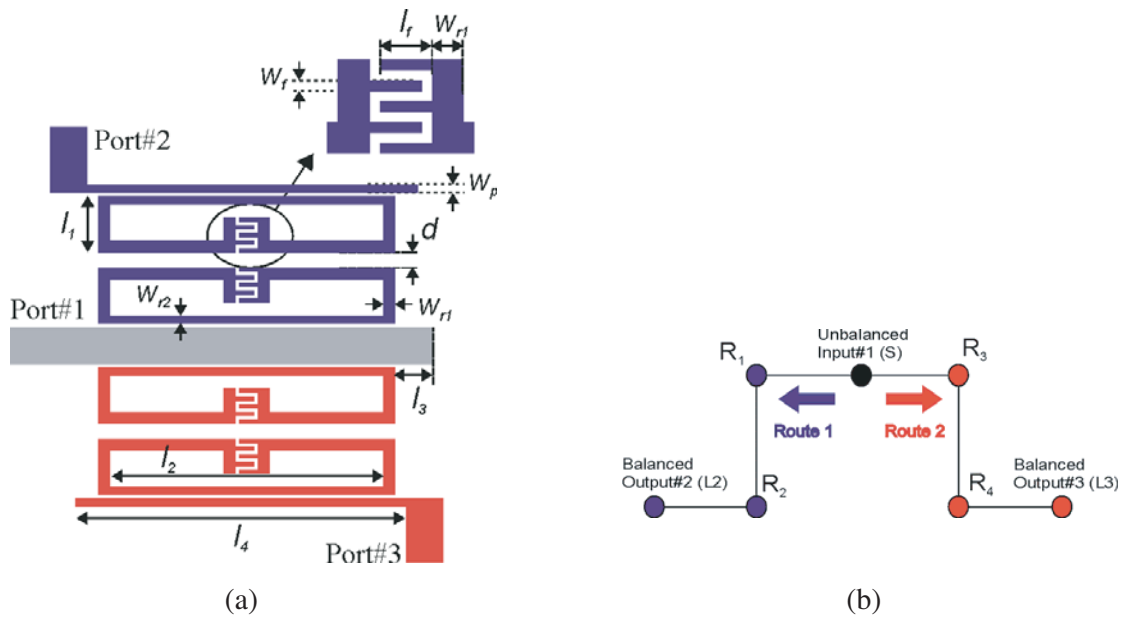


Figure 2. (a) Layout of the designed microstrip balun BPF, (b) coupling scheme.

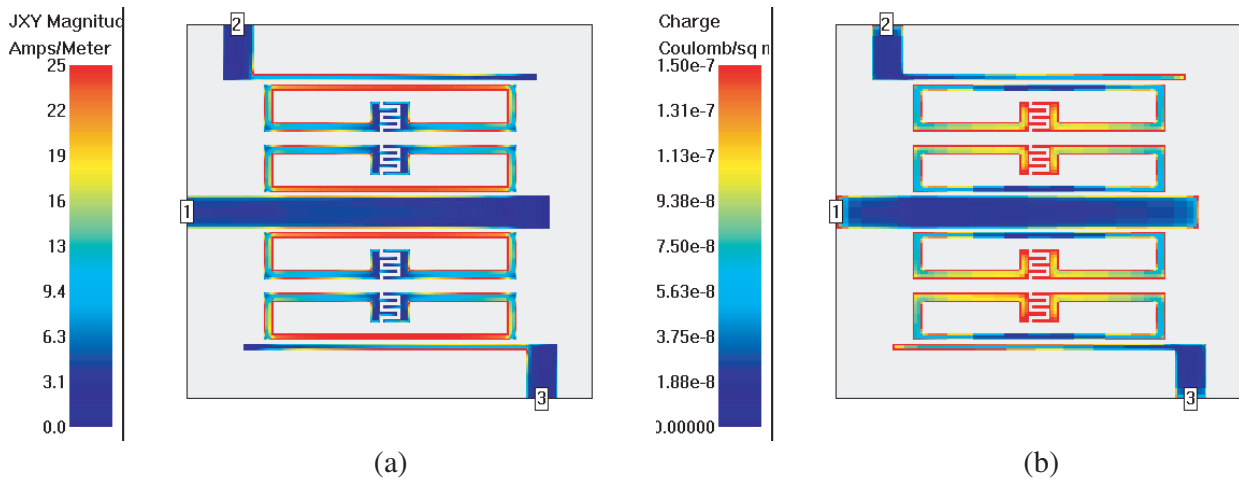


Figure 3. (a) Current distribution of the proposed structure, (b) Charge distribution of the proposed structure.

of the proposed topology is reciprocally located balanced ports which is practically useful for system integration.

A simple design methodology can be explained as follows:

1. Firstly, decide the passband center frequency of the balun bandpass filter. Since it can be derived from the odd mode resonance frequency, resonator dimensions can be found from the numerical solution of the odd mode input impedance of the proposed resonator as described in Section 2.1.
2. In order to obtain two poles inside the passband, locate one more resonator at an arbitrary distance to the first one. The exact distance between the resonators is going to be assigned after the final topology for the balun bandpass filter due to the desired bandwidth value.
3. In order to design the balun bandpass filter, two identical predefined resonators have to be coupled to an output port, and the other resonators have to be coupled to another output port. Port locations have to be determined so as to obtain 180° phase difference between the output ports as shown in Fig. 2(a) in a similar manner with [7].
4. After deciding the exact topology as shown in Fig. 2(a), different optimizations have to be realized as explained below.
 - Firstly, number and lengths of interdigital fingers have to be reassigned by an optimization in order to adjust the center frequency to the desired value exactly. Center frequency controlling mechanism with respect to the changes in the number and lengths of interdigital fingers is also demonstrated in Figs. 4(a) and 4(b).
 - After that, distances between the resonators have to be assigned depending on the desired bandwidth value.
 - Finally, lengths of l_3 and l_4 have to be found by another optimization. In this case, optimization goals are minimum phase difference and magnitude difference.

The designed balun BPF is simulated by using a Full-Wave Electromagnetic Simulator [12]. Dimensions of the designed circuit are given in Table 1. All gaps between the transmission lines in the whole structure are adjusted to 0.2 mm. An RT/Duroid substrate with a dielectric constant of 6.15 and thickness of 1.27 mm is used in all simulations and experimental studies. The designed structure allows controlling center frequency and bandwidth. During these control processes, it is desired to observe negligible changes in phase and magnitude imbalances. The center frequency can be controlled by only changing capacitances of interdigital capacitors. Thus, center frequency can be controlled without changing the total resonator dimensions or total circuit size. As mentioned in the previous section, coupled mode of the open loop resonator is odd mode since the interdigital capacitors can only affect this mode. In other words, center frequency control can be achieved by changing the odd modes of the open loop resonators. Center frequency control of the proposed balun BPF is illustrated

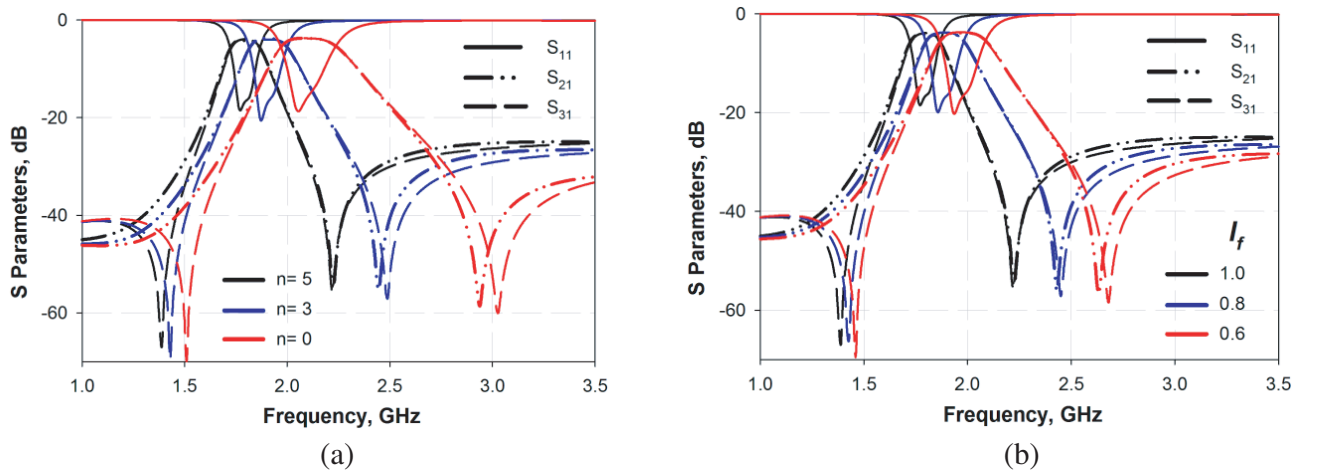


Figure 4. Center frequency control depending on the change in (a) interdigital finger number, (b) interdigital finger length.

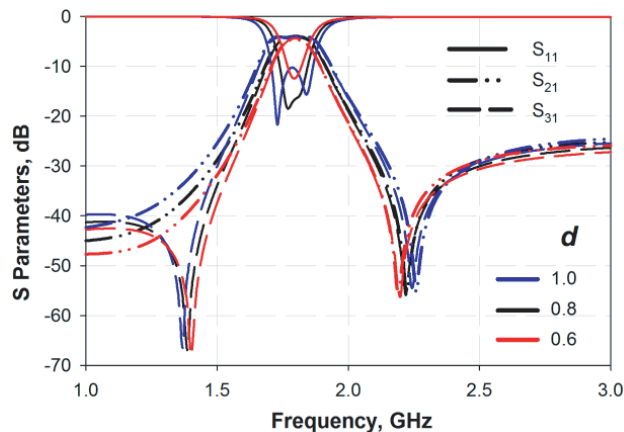
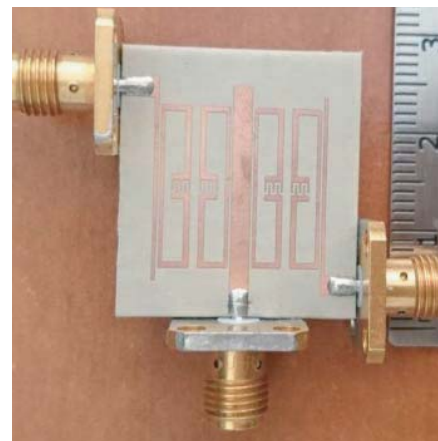
Table 1. Dimensions of the proposed balun BPF (units: mm).

l_1	l_2	l_3	l_4	l_f	w_{r1}	w_{r2}	w_f	w_p
2.9	14.2	2.0	17.2	1.0	0.6	0.4	0.2	0.4

in Figs. 4(a) and 4(b) according to the changes in finger number and finger length, respectively. A wide center frequency control range such as between 1.7 GHz and 2.1 GHz can be achieved. During the center frequency control processes, the magnitude imbalance is observed as better than 0.35 dB and phase imbalance is better than $180 \pm 5^\circ$. Insertion loss inside the passband is better than $3 + 1.2$ dB during center frequency control process.

It should be noted from Fig. 4 that there are two transmission zeros at S_{31} , and there is only one transmission zero at S_{21} . Actually the transmission zero located at the upper side of the passband results from the characteristic of the proposed resonator, since the proposed resonator exhibits the main characteristics of a conventional open loop resonator. In such a resonator, it is difficult to control the transmission zero independently. On the other hand, as can be seen from S_{31} , an extra transmission zero occurs in the lower frequencies. It actually depends on the port locations. Thus, 180° phase difference can be observed based on the output port arrangements. In such a structure, both of the transmission zeros cannot be controlled without ruining the passband performance.

Bandwidth of the passband can also be controlled depending on the coupling between the resonators. Since the resonators are coupled to each other capacitively, and bandwidth is changed while the interdigital capacitors are adjusted. In interdigital capacitors, bandwidth of the passband can also be controlled by changing the distance between the resonators. Bandwidth control is demonstrated in Fig. 5 according to the change in d . As the illustration at a center frequency of 1.8 GHz, it can be controlled between 50 MHz and 150 MHz. In this case, return losses are always better than 10 dB. During the bandwidth control processes, the magnitude imbalance is observed as better than 0.35 dB, and phase imbalance is better than $180 \pm 5^\circ$. Insertion loss inside the passband is better than $3 + 1.6$ dB during bandwidth control process. On the other hand, return losses are always obtained as better than 10 dB. The designed structure also has a clean upper stopband approximately until 4.5 GHz.

**Figure 5.** Bandwidth control according to the change in d .**Figure 6.** Photograph of the fabricated balun BPF.

3. EXPERIMENTAL RESULTS

Designed balun BPF was fabricated for the experimental verification of the proposed approach. A photograph of the fabricated structure is shown in Fig. 6. Measurements were realized by Agilent

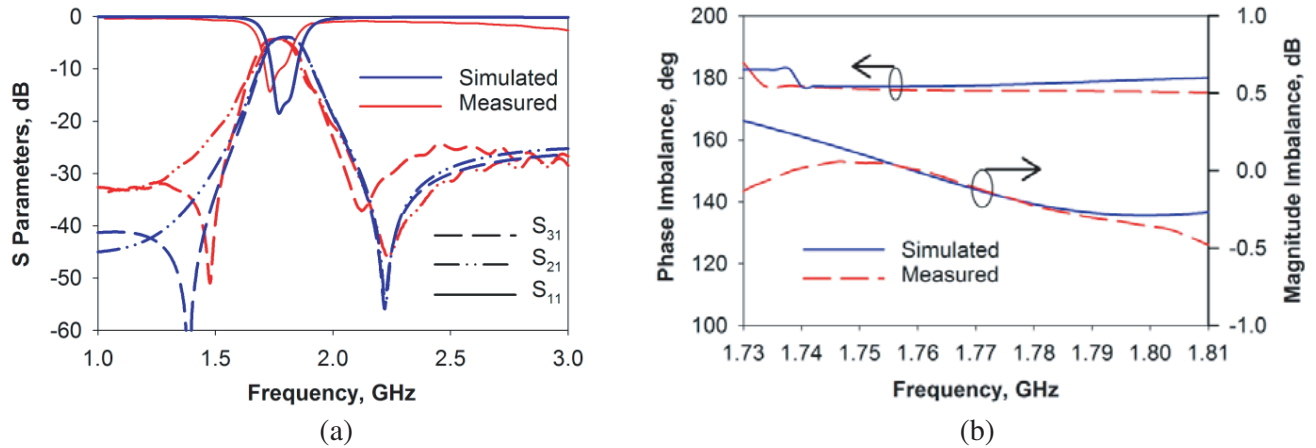


Figure 7. Comparison of the measured and simulated results, (a) for S parameters, (b) for magnitude imbalance and phase imbalance.

E5071C Network Analyzer. 50 ohm SMA connectors were used to implement the unbalanced input and balanced output ports. In the fabricated balun BPF, finger lengths and number of interdigital capacitors are chosen as 1 mm and 5, respectively. Total circuit size including 50 ohm input and output ports is $22.5 \times 22.9 \text{ mm}^2$, which corresponds to $0.135\lambda_0 \times 0.137\lambda_0$ ($0.0185\lambda_0^2$), where λ_0 is the free-space wavelength at 1.8 GHz. Comparisons of the simulated and measured results are depicted in Fig. 7. In Fig. 7(a), measured and simulated S parameters of the designed balun BPF are shown. Magnitude and phase imbalance comparisons are shown in Fig. 7(b). The measured insertion loss was measured as $3 + 1.3 \text{ dB}$, whereas the measured in-band return loss was measured as better than 10 dB. Center frequency of the passband was measured at 1.77 GHz. Fractional bandwidth of the passband is 8.3%. There are two transmission zeros for the second balanced output located at 1.47 GHz and 2.11 GHz. Transmission zero of the third balanced output was measured at 2.21 GHz. Magnitude imbalance is within 0.5 dB between 1.73 and 1.81 GHz, and it is about 0.15 dB at the center frequency. Phase imbalance was measured within $180 \pm 5^\circ$. As can be seen from Figs. 7(a) and 7(b), the simulated and measured results show a good agreement. The proposed study has a simple center frequency control mechanism for a microstrip balun BPF having high performances.

4. CONCLUSION

A novel microstrip balun BPF was designed and simulated with high performances. The designed structure has been constructed by using interdigital capacitor loaded open loop resonators. Analysis of the proposed resonator was realized by means of even and odd mode input impedances. Coupling routes of the balun BPF were also described. The designed structure has a practical center frequency control mechanism by means of interdigital capacitors. The designed circuit was also fabricated and measured to verify the proposed model. Phase and magnitude imbalances inside the passband were measured within $180 \pm 5^\circ$ and 0.5 dB, respectively. The measured and simulated results show an acceptable agreement.

ACKNOWLEDGMENT

This work was supported by the Scientific and Technological Research Council of Turkey (TUBITAK) under Grant 116E864.

REFERENCES

1. Kang, S. J. and H. Y. Hwang, "Ring-balun-bandpass filter with harmonic suppression," *IET Microwaves, Antennas & Propagation*, Vol. 4, No. 11, 1847–1854, Nov. 2010.

2. Jung, E. Y. and H. Y. Hwang, "A balun-BPF using a dual mode ring resonator," *IEEE Microwave and Wireless Components Letters*, Vol. 17, No. 9, 652–654, Sep. 2007.
3. Sun, S. and W. Menzel, "Novel dual-mode balun bandpass filters using single cross-slotted patch resonator," *IEEE Microwave and Wireless Components Letters*, Vol. 21, No. 8, 415–417, Aug. 2011.
4. Gorur, A., "Description of coupling between degenerate modes of a dual-mode microstrip loop resonator using a novel perturbation arrangement and its dual-mode bandpass filter applications," *IEEE Trans. Microw. Theory Tech.*, Vol. 52, No. 2, 671–677, Feb. 2004
5. Huang, F., J. Wang, and L. Zhu, "A new approach to design a microstrip dual-mode balun bandpass filter," *IEEE Microwave and Wireless Components Letters*, Vol. 26, No. 4, 252–254, Apr. 2016.
6. Kang, W., H. Wang, C. Miao, C. Tan, and W. Wu, "A high performance balun bandpass filter with very simple structure," *Progress In Electromagnetics Research Letters*, Vol. 31, 169–176, 2012.
7. Chen, C. M., S. J. Chang, S. M. Wu, Y. T. Hsieh, and C. F. Yang, "Investigation of compact balun-bandpass filter using folded open-loop ring resonators and microstrip lines," *Mathematical Problems in Engineering*, Vol. 2014, 1–6, Article ID 679538, 2014.
8. Xu, J. X., X. Y. Zhang, and X. L. Zhao, "Compact LTCC balun with bandpass response based on Marchand balun," *IEEE Microwave and Wireless Components Letters*, Vol. 26, No. 7, 493–495, Jul. 2016.
9. Tsai, C. L. and Y. S. Lin, "Analysis and design of new single-to-balanced multicoupled line bandpass filters using low-temperature co-fired ceramic technology," *IEEE Trans. Microw. Theory Tech.*, Vol. 56, No. 12, 2902–2912, Dec. 2008.
10. Wu, L.-S., Y.-X. Guo, J.-F. Mao, and W.-Y. Yin, "Design of a substrate integrated waveguide balun filter based on three-port coupled resonator circuit model," *IEEE Microw. Wireless Compon. Lett.*, Vol. 21, No. 5, 252–254, May 2011.
11. Hong, J. S. and M. J. Lancaster, *Microstrip Filters for RF/Microwave Applications*, Wiley, New York, 2001.
12. Sonnet User's Manual, Version 16, *Sonnet Software*, North Syracuse, NY, 2016.